Polyelectrolyte Nanoring Structures: Critical Parameters Governing Formation and Structural Analysis

Héctor Flores,[†,⊥] J-Luis Menchaca,[‡] Ferdinando Tristan,[§] Csilla Gergely,[⊥] Elías Pérez,[‡] and Frédéric J. G. Cuisinier*[,⊥]

Facultad de Estomatología, Instituto de Física, and CIEP Facultad de Ciencias Químicas, Universidad Autónoma de San Luis Potosí, Alvaro Obregón 64, 78000 San Luis Potosí, S.L.P., México, and INSERM U 595, Fédération Recherche Odontologique, Université Louis Pasteur, 11 rue Humann, 67085 Strasbourg Cedex, France

Received September 1, 2004; Revised Manuscript Received November 5, 2004

ABSTRACT: Recently we have presented new polyelectrolyte nanoring structures formed by self-assembly of poly(ethylenimine) and poly(sodium 4-styrenesulfonate) during sequential adsorption observed by AFM microscope in liquid cell technique. In this work, filter pore size and carbonate ion concentration are identified as critical parameters for their formation. We show how these two parameters modulate the nanorings formation as a consequence of the hydrophobic polyelectrolyte domains formed into the polyelectrolyte solutions and the screening effect produced by the divalent carbonate ions present also in solutions. Also, we prove how the nanorings size is controlled through competition between electrostatic and hydrophobic interactions where the charge density of the substrate plays an important role.

Introduction

Self-assembled polyelectrolyte films on surfaces have attracted much attention during the past decade for their potential in technological and biological applications.[1] Their buildup is based on first principles: dissociation of polyelectrolyte in aqueous solution releases counterions leaving ionized groups along the polymer chain.[2] These polyelectrolytes are then adsorbed onto the charged surface, producing a charge inversion at the surface that promotes the adsorption of a second charged polyelectrolyte of opposite electrical charge.[3] Alternating adsorption of anionic and cationic polyelectrolytes produces multilayer films having a fine control on film architecture and thickness.[4] Surface structure of the polyelectrolyte film is an important property for any application and evidently depends on factors such as the polyelectrolyte hydrophobic nature, substrate charge density, pH, and ionic strength. In the past, scanning electron microscopy (SEM)[5] and atomic force microscopy (AFM)[6] have been used to observe film surface structure. However, pretreatment of samples prior to observation limits these techniques. Alternatively, liquid-cell AFM was recently proposed as an in situ technique to monitor the surface during the self-assembly of the film to avoid preparation artifacts.[7] This technique has revealed the presence of nanoring like structures in the surface after successive adsorption of poly(ethylenimine) and poly(sodium 4-styrenesulfonate) polyelectrolytes.[8] Potential applications are envisaged for this novel structure such as specific ligand for protein immobilization, calcium phosphate nucleation centers, and nanopatterning. The formation of these nanorings depends on different experimental conditions that also determine the behavior of the polyelectrolytes in solution. It has been observed that nanoring formation depends on the presence of carbonate ions and polyelectrolyte filtration in their preparation.[8] The former is related to the screening effects produced by carbonate ions present in solution, while the latter is precisely associated with the presence of polyelectrolyte domains in solution.[9] The screening was demonstrated in early reports of ionic specificity in polyelectrolytes in the presence of different salts NaCl, $CaSO_4$, and $CaCl_2$.[10] Monovalent anions had little effect on polyelectrolytes, but when the valence was changed from monovalent to divalent the effect was much larger.[11] It has also been recognized that two like-charged polyelectrolytic attractions are mediated by their counterions. The fluctuation and correlation of these counterions explain the attraction between like-charged polyelectrolytes.[12]

On the other hand, domain formation is a typical property of hydrophobic polyelectrolytes in water. The shape of hydrophobic polyelectrolytes is determined by the competition between electrostatic and hydrophobic interactions. The hydrophobic interactions induce polymer chain collapse into a spherical globule, minimizing the number of unfavorable monomer−water contacts, while electrostatic interactions force the polymer chain to stretch to minimize the electrostatic repulsion between charged monomers. The ability of polyelectrolytes to assume a globular conformation was first recognized and described by Liquori.[13] The balances of hydrophobic and electrostatic interactions result in the formation of necklace globules connected by narrow strings.[14] The presence of domains in polyelectrolyte solution has been discussed for quite a long time.[15] The pearl-necklace conformation produced by the hydrophobic polyelectrolytes was theoretically predicted[16] and confirmed by small-angle neutron scattering (SANS) experiments[17,18] and fluorescence emission of hydrophobic regions (or pearls) labeled by pyrene.[19] Domains are found in a large variety of polyelectrolytes with different chemical structure.[6] Such domains may be related to the internal structure of the nanorings. Alternatively, dynamic light

[†] Facultad de Estomatología, Universidad Autónoma de San Luis Potosí.
[‡] Instituto de Física, Universidad Autónoma de San Luis Potosí.
[§] CIEP Facultad de Ciencias Químicas, Universidad Autónoma de San Luis Potosí.
[⊥] Université Louis Pasteur.
* Corresponding author: Tel + (33) 390 24 33 74, Fax + (33) 390 24 33 79; e-mail fred.cuisinier@odonto-ulp.u-strasbg.fr.

10.1021/ma048212u CCC: $30.25
Published on Web 12/30/2004

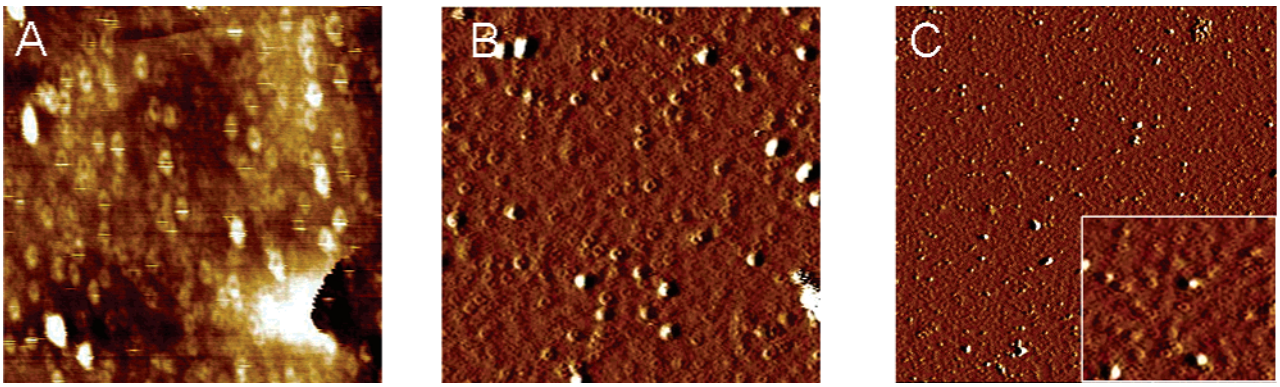

Figure 1. Nanoring obtained with polyelectrolyte solutions filtered with a 0.22 μm filter and different exposure times to air: (A) nanorings obtained after 24 h with an external diameter (D) of 420 ± 22 nm; (B) after 12 h, D = 309 ± 27 nm; (C) after 3 h, D = 187 ± 8 nm. Scan size for all images is 10 × 10 μm^2; a zoom of 5 × 5 μm^2 is also shown in (C).

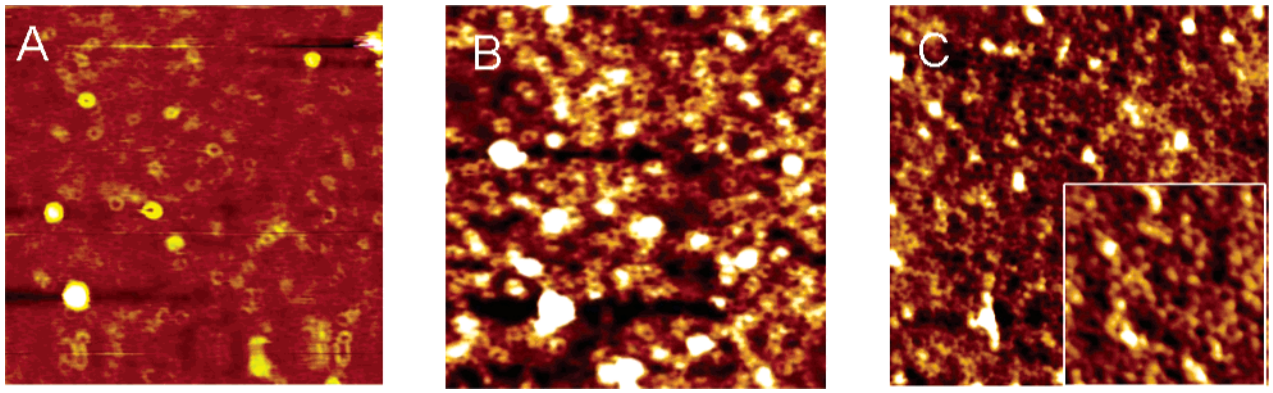

Figure 2. Nanoring obtained with filtered polyelectrolyte solutions at an exposure time of 3 h: (A) filter of 0.45 μm in pore size gives nanorings of 731 ± 50 nm in external diameter; (B) filter of 0.22 μm gives D = 413 ± 27 nm; (C) filter of 0.10 μm gives D = 213 ± 32 nm. Scan size for all images is 10 × 10 μm^2; a zoom of 5 × 5 μm^2 is also shown in (C).

scattering experiments have shown that solution filtering process determines polyelectrolyte domains size in solution.[20] Indeed, no spontaneous reversible process was observed, indicating that the new size distribution is relatively stable after this mechanical treatment. Adsorbed polyelectrolytes form different surface patterns depending on their hydrophobic nature and on the interaction between the adsorbed molecules and the substrate and also on the intermolecular interactions. AFM experiments have already revealed the formation of domains when hydrophobic molecules were adsorbed in silica substrate.[21]

Taking into account the existing works about polyelectrolyte conformation in solution, we investigate how the filter pore size and carbonate ion concentration in solution modulate the formation of these new polyelectrolyte nanoring structures.

Materials and Methods

AFM Microscope Observation. A liquid cell is used to obtain in situ contact mode AFM images with a Nanoscope IIIa AFM microscope (Digital Instruments Santa Barbara, CA). Cantilevers with a spring constant of 0.03 N/m (MLCT-AUHW, Park Scientific) are used, following tips silanization with octadecyltrichlorosilane (OTS, 95%, Aldrich) to turn them hydrophobic. Height and friction images at 1 Hz scan rate with a resolution of 512 × 512 pixels, at 5, 10, and 20 μm scanning, were captured simultaneously; only the height images are reported.

Glass Support Preparation. Glass slides of 14 mm diameter (Micro Cover Glass, France) were previously cleaned with Hellmanex solution at 3%, heated at 60 °C for 15 min, and then rinsed with water. Afterward, the glass slides are cleaned in 1% H_2SO_4 solution for 15 min at 60 °C. Finally, they are rinsed and dried.

Polyelectrolytes and Buffer Solution Preparation. Polyelectrolyte solutions are prepared using poly(ethylenimine) (PEI) ($M_w \approx 7 \times 10^4$ Da) and poly(sodium 4-styrenesulfonate) (PSS) ($M_w \approx 7 \times 10^4$ Da both from Sigma, France) at 1 mg/mL concentration in water. Tris(hydroximethyl)aminomethane (TRIS, 25 mM), 2-(*N*-morpholino)ethanesulfonic (MES, 25 mM), and NaCl (100 mM) (all from Sigma) are used to prepare the buffer solution (TRIS-MES) at pH 7.4. All solutions are prepared with degassing ultrapure water (Mill Q-Plus system, Millipore) with a resistivity of 18.2 MΩ cm (Millex PVDF, Millipore). A high-vacuum pump (Pascal 2010 SD, ALCATEL, France) at 2 × 10^{-3} mbar per 25 min was used for degassing the water. Polyelectrolyte solutions were kept in contact with air for 3, 12, and 24 h in order to increase carbonate concentration and filtered with 0.10, 0.22, or 0.45 μm pore size filters.

Self-Assembly Polyelectrolytes Process. Following buffer injection into the AFM liquid cell, an image of the glass surface is taken as reference. The positive polyelectrolyte PEI solution is then injected and let in contact with the substrate for 15 min and then rinsed with 5 mL of buffer, and then the PEI film is imaged. Negative polyelectrolyte PSS is then injected and let for 15 min in contact with PEI film followed rinsing with 5 mL of buffer solution.

All statistical analyses were performed with SigmaStat v2.03 (SPSS Inc., Chicago, IL).

Results and Discussion

In Figure 1, we observe different nanoring sizes depending on the exposure time to air with a fixed filter pore size of 0.22 μm, while in Figure 2 nanoring sizes is depending of filter pore size with a fix exposure time

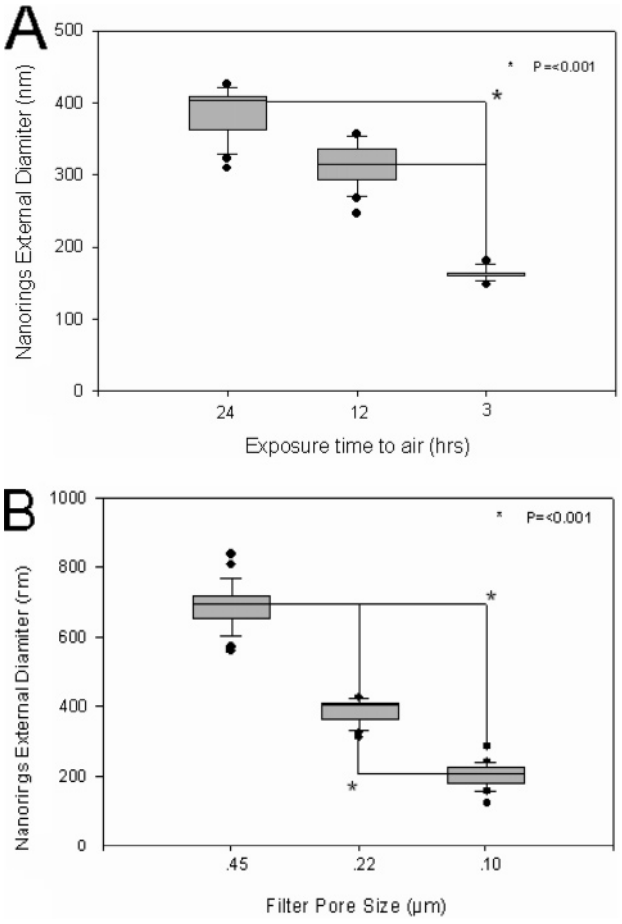

Figure 3. (A) Exposure time to air. Statistical difference ($p \leq 0.001$) is denoted by an asterisk. (B) Nanoring external diameter as a function of filter pore size. p = probabilities as numbers in the interval from 0 to 1 assigned to events whose occurrence or failure to occur is randomly calculated.

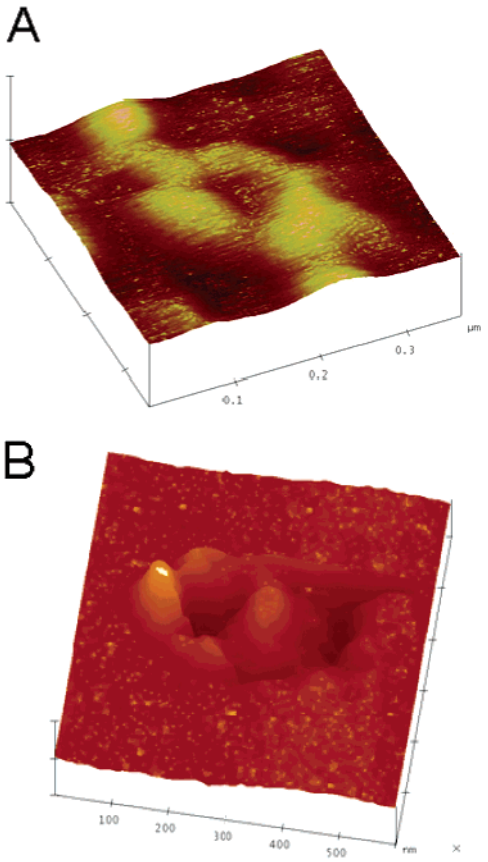

Figure 4. Domains are also present in the nanoring structure. (A) Nanoring formed by 5 globular domains (image size of 400 × 400 nm^2, $Z = 5$ nm). (B) Nanoring formed by four globular domains (image size of 600 × 600 nm^2, $Z = 15$). Approximate external diameter is 100 and 340 nm in (A) and (B), respectively.

to air of 3 h. From these images, we can observe that the nanoring distribution is homogeneous on the surface, and the nanoring size is nearly constant in each case.

We analyzed the film and nanoring dimensions using Nanoscope software. A statistical analysis was performed in 10 experiments (taking more than 10 nanorings by experiment) representing the different preparation conditions. External diameters as a function of exposure time to air and filter pore size are shown in parts A and B of Figure 3, respectively.

The results show a significant statistical difference in the external diameters among the nanorings obtained in all the cases ($p \leq 0.001$). Larger exposure time to air produce nanorings with a bigger average diameter. Using filter pore size of 0.22 μm, after 24, 12, and 3 h we obtain nanorings of 420 ± 22, 309 ± 27, and 187 ± 8 nm in external diameter, respectively. Equivalently, large pore filters of 0.45 μm produce nanorings with an average diameter of 731 ± 50 nm; nanorings are bigger than those formed with filter of 0.2 μm giving 413 ± 27 nm and 0.1 μm giving 213 ± 32 nm. In all the experiments the nanoring external diameter dispersion is less than 18%, indicating a relatively narrow nanoring distribution.

The measured roughness (Ra value) of glass and PEI surfaces, respectively 0.15 and 0.17 nm, are approximately equal and very flat in all the analyzed images. This indicates that a homogeneous layer of PEI is formed on the glass surface. After PSS adsorption, roughness increases from 0.5 to 9 nm, depending on the nanoring size. This increase should be related to domains of the PSS in solution. Such domains are present in PSS solution and are adsorbed on PEI film. PSS is hydrophobic and PEI is hydrophilic, and their characteristic properties in solution must be reflected in the polyelectrolyte film. PEI and PSS are adsorbed at low ionic strength because they are dissolved in water. Therefore, PEI on a charged surface leads to semispherical domains that are compressed and coalesced to produce a flat, homogeneous film with homogeneous density charge on the surface.[22] The necklace conformation of the PSS in solution forms domains that are adsorbed on PEI layer increasing film roughness. Figure 4 shows the structure of two nanorings formed by a series of domains. They should be related to PSS domains in solution whose form and size have to be modified by the charged surface and PEI film.

The number of domains observed in our experiments is typically five or four whatever the experimental conditions. The size of these domains depends on the filter pore size used during polyelectrolyte filtration. Polyelectrolyte domains in solution are initially present and after filtration they are modified.[23] Retention based on the size exclusion does not represent the main mechanism.[13] This change could be associated with the collapse and coalescence of many domains into a bigger one when they are passing through the pore of the filter producing specific domains with homogeneous size after

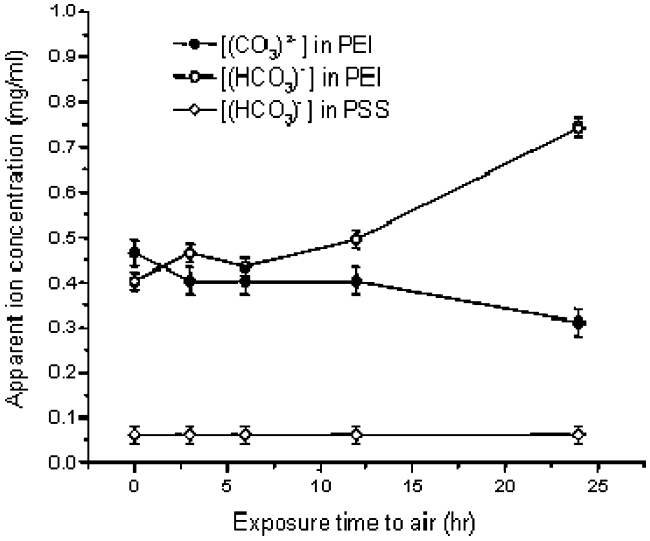

Figure 5. Carbonate ion species present in PEI and PSS solutions. The concentration of divalent ions decreases while the monovalent ion concentration increases through time in PEI solution. PSS solution does not contain divalent ions, and monovalent ion concentration is constant through time.

filtering.[12] As a general rule, larger filter pore size produces larger polyelectrolyte domains. The homogeneous size distribution of PSS domains in solution after filtering is therefore related to the homogeneous size of the domains present in the nanorings that are also homogeneous in consequence.

Concentration of divalent ions is the second parameter studied (Figure 3A). It is well-known that aqueous solutions adsorb CO_2, forming monovalent (HCO_3^-) and divalent ions (CO_3^{2-}) ions depending on the pH of the solution.[24] To know how the carbonate ions are accumulating in the PEI and PSS solutions, titration experiments were done. Methyl orange and phenolphthalein are used as indicators to determine the concentration of monovalent and divalent ions by titration, respectively. Ion concentration is related to the volume of HCl spent to react with each kind of ion producing a color change. The results are show in Figure 5.

The PEI and PSS solutions are exposed to air, and samples are taken at 0, 3, 6, 12, and 24 h. It is assumed an additive contribution of the polyelectrolyte concentration because they are titrated at the same time that the carbonate species; therefore, results are expressed like apparent ion concentration. Taking the latter into account, we can observe that the HCO_3^- apparent concentration is increasing with time in the PEI solution while the CO_3^{2-} apparent concentration is decreasing. On the other hand, divalent ions are not detected in PSS solutions, and the HCO_3^- apparent concentration is constant. This behavior is showing the mechanism of screening in the PEI molecules. When PEI is dissolved in water, the amine groups in the polyelectrolyte molecules gain protons immediately, giving a positive net charge to the PEI molecule. After a few hours, the quantity of the CO_3^{2-} ions decreases and HCO_3^- concentration increases. This occurs because the protons in the amine groups capture the CO_3^{2-} ions forming HCO_3^- ions. This phenomenon screens the positive charge of the PEI molecules, making it weaker. On the contrary, this phenomenon does not occur in the PSS solution due to the negative charge of the PSS molecule. It can be deduced from these evidences that the ions

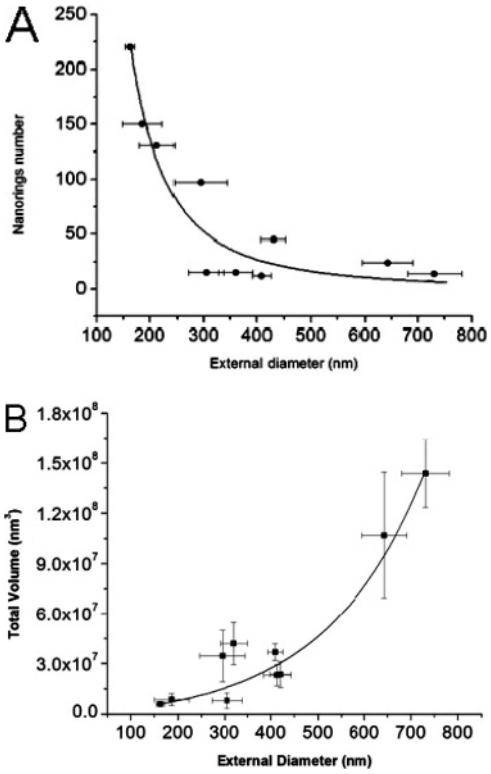

Figure 6. (A) Nanoring number decrease with nanorings external diameter increase (D). Data obtained from images of 5×5 μm^2; solid line represents the fit of the function $y = b + a/D$ with $b = 0.194654$ and $a = -293.59$. (B) However, total volume increases with D, confirming a screening electrostatic effect. The lines are a guide to the eye.

modulate the electrostatic interaction between the PEI layer and PSS domains during adsorption. These results suggest that the effect of both carbonate ions on nanoring size is mediated trough PEI. The fact that the divalent ions concentration decreases vs time in PEI solution indicates that the presence of this ion is coupled with a size increase of nanoring (see Figures 1 and 3A). We have previously observed a screening effect; at high divalent ion concentration nanorings have a weak adhesion to the surface and are unstable on the surface.[8] We can deduce that the carbonate ions modulate the electrostatic interaction between PEI layer and PSS domains during adsorption.

When the images were analyzed by number of nanorings per surface, we also find that the number of nanorings per surface unit is strongly dependent on size (Figure 6A). When the size of the ring increases, the number of nanorings per surface decreases. We also show in the Figure 6B that the total volume occupied by the nanorings increases with their size.

This confirms the fact that the electrostatic repulsion between polyelectrolyte domains and the charge density of the surface both are strongly related with the formation and size of the nanoring. Additionally, the mean surface coverage is approximately to $18 \pm 11\%$ for all the nanorings reported here. Despite this broad distribution, the surface coverage is far away from the maximum surface coverage obtained for a random sequential adsorption (RSA) process that gives a value equal to 54.7%.[25] This indicates again the important role of electrostatic interactions in the formation of the nanorings.

Analysis of nanorings dimensions gives us additional information. We show a three-dimensional image in

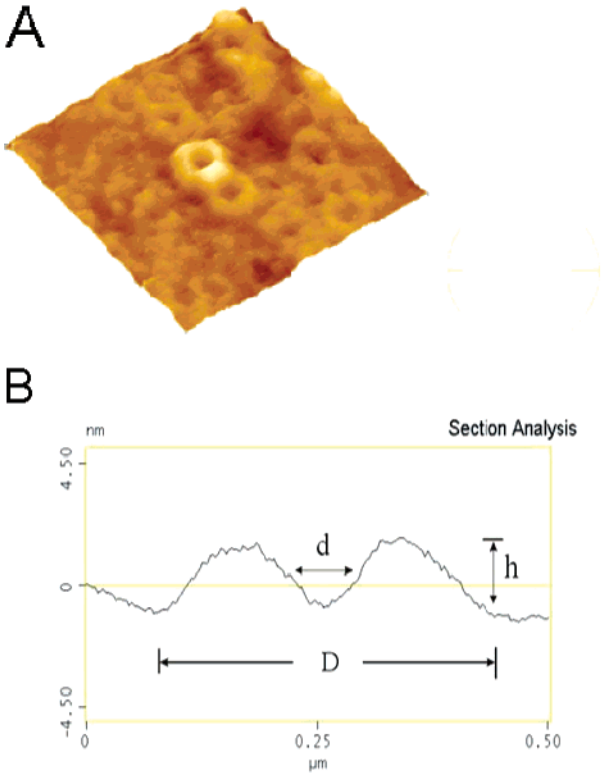

Figure 7. (A) Nanorings details in a 3-D image (scan size 2.5 × 2.5 μm^2; Z = 15 nm). (B) Definition of the external diameter (D), the internal diameter (d), and the height (h) of the nanorings using a transversal section.

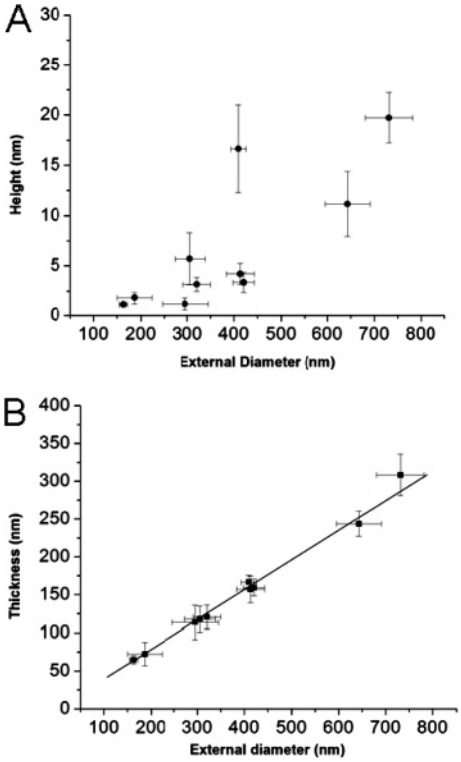

Figure 8. (A) Screening effect is correlated between height and nanoring external diameter. (B) Linear behavior between thickness and external diameter for the nanorings. This indicates uniform nanoring growth that justifies a constant value for the ratio between internal and external nanoring diameter of 23 ± 5%.

Figure 7A, and height (h) as well as external and internal diameter (D and d, respectively) are represented schematically in Figure 7B in a profile section.

The thickness, defined as $^1/_2(D - d)$, and the height of the nanorings with the external diameter are shown in parts A and B of Figure 8, respectively, where we can remark that external diameter of nanorings is ranging from 180 to 730 nm and height is always of few nanometers (2−20 nm).

It shows that when the size of the nanoring increases, the thickness and height also increase; however, it is very remarkable. The linear dependence between the thickness and the external diameter indicates a uniform nanoring growth. Statistical analysis of these results shows that the ratio between external and internal nanoring diameter for all experiments is roughly constant. The internal diameter represents 23 ± 5% of the external diameter in all the cases.

The fact that the diameter ratio is nearly constant whatever the experimental conditions raises many hypothesis. It confirms that nanorings size is dependent on domains size. Large domains form large nanorings with always the same proportional core in the center of nanoring. It can be related either by steric hindrance or by repulsion between domains. Such repulsion should be proportional to domain size in order to keep the ratio constant. This is indicative that the polyelectrolytes conformation in solution could be the base of nanorings formation, and it is always an invariable mechanism in the range of the experimental conditions. Therefore, nanorings are formed by polyelectrolyte domains present in solution with almost uniform size when these are adsorbed on the surface give to nanorings a domain structures. This mechanism is not far from formation of micelle structures for the polyelectrolytes complex.[26,27]

Conclusion

In this paper, we show that the formations of nanoring structures are governed by two critical parameters: filter pore size and carbonate ions concentration in the polyelectrolyte solutions. The filtering of PSS forms a homogeneous size of polyelectrolyte domains in solution, and they are also present in the structure of the nanorings. Additionally, the accumulation of carbonate ions in PEI layer modulates the electrostatic interaction, producing large nanorings as polyelectrolyte solution is exposed to air. The balances between hydrophobic and electrostatic forces define therefore the structure and size of the nanorings. However, it is no possible to determine where hydrophobic and hydrophilic portion in the nanoring structure are. Evidently, additional experimental and theoretical work is necessary to understand nanorings formation. Applications such as protein immobilization or nanopatterning can be also envisaged for this novel structure. The experimental results presented in this work can be useful for these purposes.

Acknowledgment. This work was partially supported by the "Biomolecular Materials Project": CONACYT-Mexico (ER026), Mexico-France Program: SEP−CONACYT-ANUIES-ECOS France (M01-S01) and PROMEP, Mexico. J.L.M. and F.T. thank Conacyt and H.F. thanks PROMEP for their PhD scholarships.

References and Notes

(1) Decher, G.; Schlenoff, J. B. *Multilayer Thin Films: Sequential Assembly of Nanocomposite Materials;* Wiley: New York, 2003.

(2) Hara, M. *Polyelectrolytes;* Marcel Dekker: New York, 1993.
(3) Decher, G.; Hong, J. D.; Schmitt, J. *Thin Solid Films* **1992**, *210*, 831−835.
(4) Decher, G. *Science* **1997**, *227*, 1232−1237.
(5) Reihs, T.; Müller, M.; Lunkwitz, K. *Colloids Surf., A* **2003**, *212*/*1*, 79−95.
(6) Caruso, F.; Furlong, D. N.; Ariga, K.; Ichinose, I.; Kunitake, T. *Langmuir* **1998**, *14*, 4559−4565.
(7) Menchaca, J. L.; Jachimska, B.; Cuisinier, F.; Perez, E. *Colloids Surf, A* **2003**, *222*, 185−194.
(8) Menchaca, J. L.; Flores, H.; Cuisinier, F.; Perez, E. *J. Phys.: Condens. Matter* **2004**, *16*, S2109−S2117.
(9) Seldak, M. *J. Chem. Phys.* **2002**, *116*, 5256−5262.
(10) Flory, P. J.; Osterheld, J. E. *J. Phys. Chem.* **1959**, *58*, 653−661.
(11) Burak, Y.; Ariel, G.; Andelman, D. *Biophys. J.* **2003**, *85*, 2100−2110.
(12) Gelbart, W. M.; Bruinsma, R. F.; Pincus, P. A.; Parsegian, V. A. *Phys. Today* **2000**, *53*, 38−44.
(13) Liquori, A. M.; Barone, G.; Crescenzi, V.; Quadrifoglio, F.; Vitagliano, V. *J. Macromol. Chem.* **1966**, *1*, 291−305.
(14) Baigl, D.; Sferrazza, M.; Williams, C. E. *Europhys. Lett.* **2003**, *62*, 110−116.
(15) Sedlak, M. *J. Chem. Phys.* **2002**, *116*, 5236−5245.
(16) Dobrynin, A. V.; Rubinstein, M.; Obukhov, S. P. *Macromolecules* **1996**, *29*, 2974−2979.
(17) Matsuoka, H.; Schwahn, D.; Ise, N. *Macromolecules* **1991**, *24*, 4227−4228.
(18) Ermin, B. D.; Amis, E. J. *Macromolecules* **1997**, *30*, 6937−6942.
(19) Eassafi, W.; Lafuma, F.; Williams, C. E. *J. Phys. II* **1995**, *5*, 1269−1275.
(20) Sedlak, M. *J. Chem. Phys.* **2002**, *116*, 5246−5255.
(21) Gunther, J.; Stupp, S. I. *Langmuir* **2001**, *17*, 6530−6539.
(22) Borisov, O. V.; Hakem, F.; Vilgis, T. A.; Joanny, J.-F.; Johner, A. *Eur. Phys. J. E* **2001**, *6*, 37−47.
(23) Sedlak, M. *Macromolecules* **1993**, *26*, 1158−1162.
(24) Drever, J. I. *The Geochemistry of Natural Water: Surface and Groundwater Environments*; Prentice Hall: Englewood Cliffs, NJ, 1997.
(25) Swendsen, R. H. *Phys. Rev. A* **1981**, *24*, 504−508.
(26) Pergushov, D. V.; Remizova, E. V.; Feldthusen, J.; Zezin, A. B.; Müller, A. H. E.; Kabano, V. A. *J. Phys. Chem. B* **2003**, *107*, 8093−8096.
(27) Buchhammer, H.-M.; Mende, M.; Oelmann, M. *Colloids Surf., A* **2003**, *218*, 151−159.

MA048212U